

Residence Time Distribution in a Size-Exclusion SMB for Insulin Purification

Sungyong Mun, Yi Xie, and Nien-Hwa Linda Wang

School of Chemical Engineering, Purdue University, West Lafayette, IN 47907

This study analyzes for the first time the residence time distribution in a size-exclusion simulated moving bed (SMB) process. In an SMB, the raffinate port is located downstream from the feed port, whereas the extract port is located upstream from the feed port. The location of the product ports and periodic port movement results in a residence time distribution that strongly depends on solute injection time. The earlier a fast-moving solute is injected during the switching period, the earlier it exits the raffinate port. In contrast, the earlier a slow-moving solute is injected during the switching period, the later it exits the extract port. Furthermore, only a fraction of the stream is drawn as the raffinate product or the extract product. The rest is recycled. The recycle results in the splitting of a differential pulse into a pulse train with diminishing magnitude. The shape of the pulse train depends on the pulse injection time. A large recycle ratio, which results from a low selectivity, causes a long decay of the pulse train and increases tailing of the residence time distribution curve. Mass-transfer effects broaden the pulse train and the residence time distribution. To shorten the residence time of a fast-moving solute, one can increase the flow rate of zone II, decrease the length of zone III, or feed during the first half of the switching period. To shorten the residence time of a slow-moving solute, one can decrease the flow rate of zone III, decrease the length of zone II, or feed during the second half of the switching period. Rate model simulations show that these strategies can significantly reduce the residence time of insulin in SMB.

Introduction

Insulin is an important therapeutic protein for the treatment of diabetics. The demand of high-purity insulin results in extensive purification steps in production. At present, insulin is separated and purified through many batch chromatography steps (Kroeff et al., 1989; Ladisch and Kohlmann, 1992). A previous study showed that the batch size-exclusion chromatography can be replaced with a tandem SMB process (two SMB units in series), which has higher yield, higher throughput, and lower mobile phase consumption (Xie et al., 2002). As shown in Figure 1, pro-insulin (HPI) is removed from the raffinate port in the first SMB (Ring I). The effluent from the extract port of Ring I is collected and loaded into the second SMB (Ring II), where insulin is separated from ZnCl_2 .

Long residence time of a protein in SMB may result in aggregation or denaturation. This possibility raises concerns

in the use of SMB for protein purification. For this reason, it is important to understand the residence time of a solute in SMB and to find effective strategies to reduce its residence time if needed.

In batch chromatography, a small pulse is dispersed by mass-transfer effects as it migrates through a column. As a result, molecules in the pulse have different residence times, or a distribution of residence times. Some solutes leave the column early, but others late. This distribution can be estimated by injecting a small pulse into the column at some time $t = 0$ and then measuring the concentration C in the effluent stream as a function of time, which is defined as the residence time distribution function (RTD) (Danckwerts, 1953).

The RTD in batch chromatography is easy to predict because there is only one product port, and the port is located at a fixed position. Moreover, all the solutes experience the same flow rate. However, in a four-zone SMB, the raffinate

Correspondence concerning this article should be addressed to N.-H. Linda Wang.

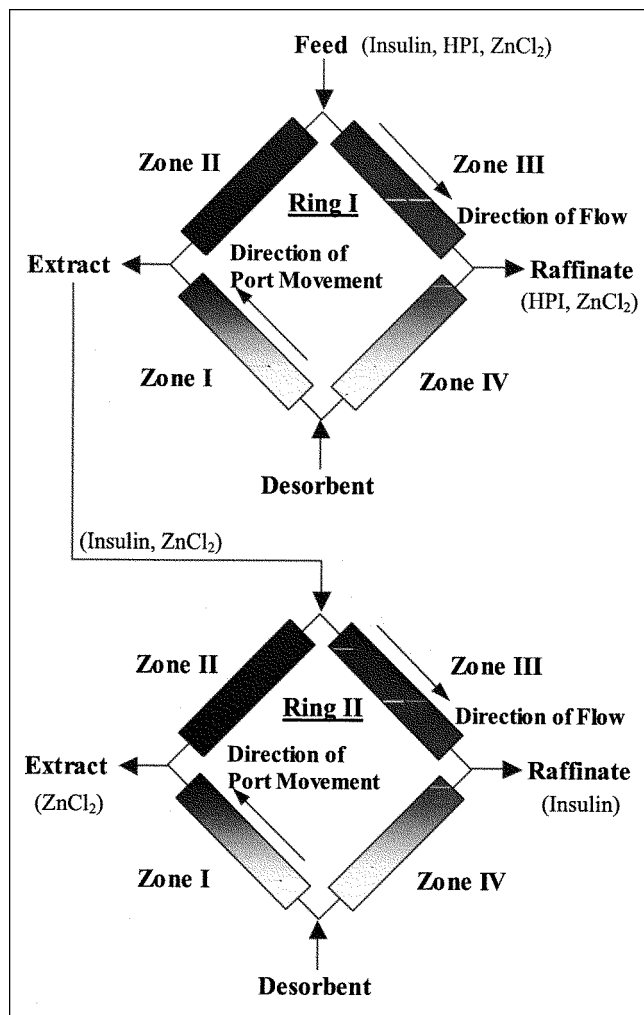


Figure 1. Tandem SMB process for insulin purification.

product port is located downstream from the feed port, whereas the extract product port is located upstream from the feed port. The ports also move periodically along the mobile phase flow direction. The four zones have different flow rates and some portion of effluent stream is recycled within the SMB. For these reasons, the RTD in the SMB is more complicated than in batch chromatography.

The major objective of this study is to clarify the residence time characteristics in an SMB process. Local equilibrium analysis is developed for systems without mass-transfer effects (ideal systems) in order to understand the effects of periodic port movement and recycle. Simulations based on a detailed rate model are then used to understand the effects of mass transfer in a nonideal system, which include axial dispersion, film mass transfer, and intraparticle diffusion. Effects of selectivity and throughput on residence time are also investigated. Based on the results of the analysis, strategies to shorten the residence time of insulin in a tandem SMB are formulated and tested using rate model simulations.

The results show that the residence time of insulin in a tandem SMB strongly depends on the injection time. In the first ring, insulin is the slow-moving solute and it is recovered

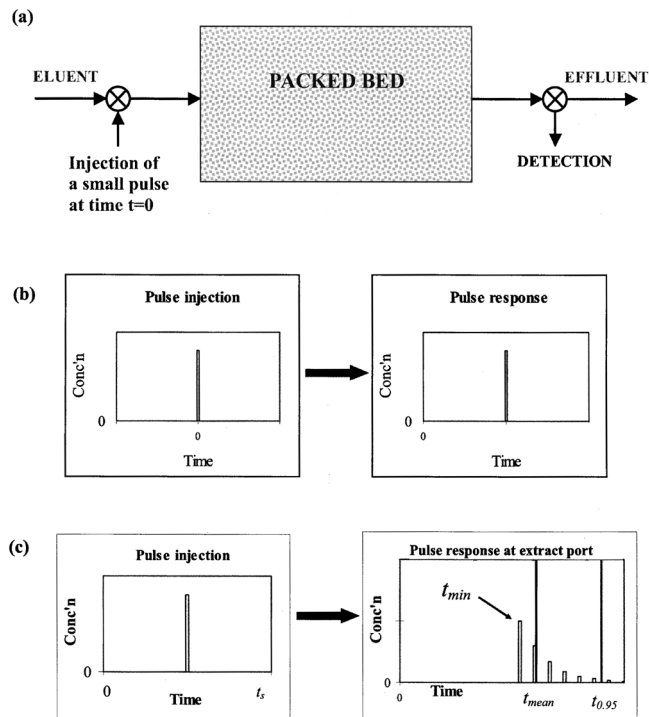


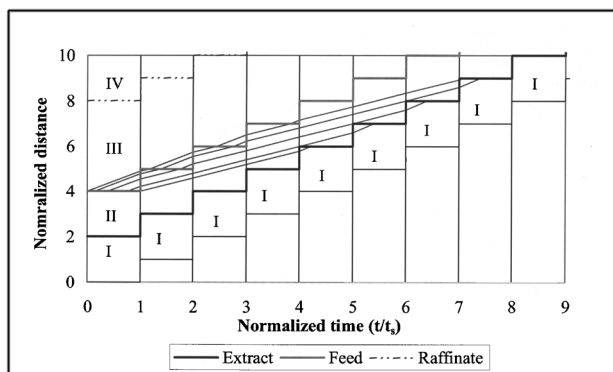
Figure 2. RTD for a pulse.

(a) RTD measurements; (b) batch chromatography without mass-transfer effects (ideal system); (c) SMB without mass-transfer effects (ideal system).

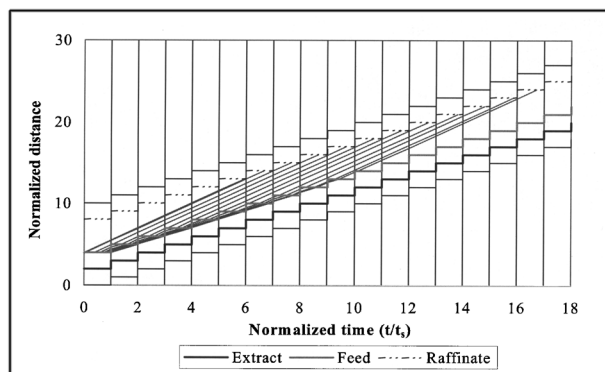
in the extract port. Since the extract port is located upstream from the feed port, the insulin injected in the second half-switching time has a shorter residence time. In the second ring, insulin is the fast-moving solute and it is recovered in the raffinate port. Since the raffinate port is located downstream from the feed port, the insulin injected in the first half-switching time has a shorter residence time. If a short residence time is required for insulin stability in SMB, such a partial feeding strategy can effectively shorten the residence time of insulin. Modifications in zone flow rates and zone length can also shorten the residence time of a solute. The zone II flow rate can be increased or the zone III length can be decreased to shorten the residence time of a fast-moving solute. The zone III flow rate can be decreased or the zone II length can be decreased to shorten the residence time of a slow-moving solute. These three strategies can be applied in combination to substantially shorten the residence time of insulin.

Theory

The amount of time a solute spends in a packed bed is the residence time of the solute. The packed bed in Figure 2a can be either a single column or a series of columns in SMB. A small pulse is used to investigate the residence time in a four-zone SMB. The pulse must be injected into the feed-stream in as short a time as possible. Not all the solutes injected into the bed have the same residence time. Many factors affect the residence time of a solute and result in a distribution of residence time. The factors include port move-



(a)



(b)

Figure 3. Solute movement diagrams from the LEA without recycle effects in Ring I ($t_s = 1804$ s).

The Y-axis is normalized by single column length ($L_c = 0.15$ m). (a) Insulin (slow-moving solute). Reduced solute velocity ($u_s \times L_c/t_s$) of insulin: 1.02 (zone I), 0.60 (zone II), 0.90 (zone III). (b) HPI (fast-moving solute). Reduced solute velocity ($u_s \times L_c/t_s$) of HPI: 1.01 (zone II), 1.51 (zone III).

ment velocity, recycle ratio, mass-transfer effects, zone configuration, selectivity, and throughput.

Two approaches are used in the analysis of RTD in SMB. In the first approach, we used a local equilibrium model based on the assumption that there is no mass-transfer effect. This simplification enables us to isolate the effects of port movement and recycle on RTD from those of mass-transfer effects.

In the second approach, we used simulations based on a detailed rate model, which takes into account mass-transfer effects, port movement, and recycle. In this model, the differential mass-balance equations with appropriate initial and boundary conditions are solved. Comparison of the results from the two approaches shows clearly the effects of mass transfer on RTD.

RTD in an ideal system

In an ideal system, there is no mass-transfer effect. Figure 2b shows that all the solute molecules have the same residence time in an ideal batch chromatography. This is because all the solutes migrate at the same velocity within the column. A four-zone SMB, on the other hand, has four periodically moving ports. The raffinate port is located downstream from the feed port. For a fast-moving solute, the earlier the injection time, which is the time that the solute is introduced into the SMB, the earlier it exits the raffinate port (or first in and first out). In contrast, the extract port is located upstream from the feed port. For a slow-moving solute, the earlier the injection time, the later it exits the extract port (or first in and last out). This point can be understood by the solute movement diagrams of SMB shown in Figure 3. Furthermore, part of the stream in zone I continues to zone II and, similarly, part of the stream in zone III continues to zone IV. Such recycle results in a distribution of residence times (or a “recycle pulse train”) even in the absence of mass-transfer effect, as shown in Figure 2c. The pulse train forms a decreasing geometric progression after t_{\min} . The shape of the pulse train depends on the pulse injection time. The decay of the pulse train occurs more slowly as more so-

lutes are recycled. These are the two major differences between the RTD in SMB and the RTD in batch chromatography. Since size-exclusion systems are linear isotherm systems, the residence time history is repeated every switching period, so that the RTD of solutes during one switching period is representative of the RTD of all other switching periods.

RTD in a nonideal case with significant mass-transfer effects

In batch chromatography, RTD does not depend on when the small pulse was injected into the column. All the pulses have the same RTD regardless of their injection times. This is why only one RTD can characterize the residence time of a solute in a batch chromatography process. However, in SMB, the small pulses injected at different times within a switching period have different RTDs, as shown in Figure 4. Notice that the pulse response in a nonideal system (Figure 4) is

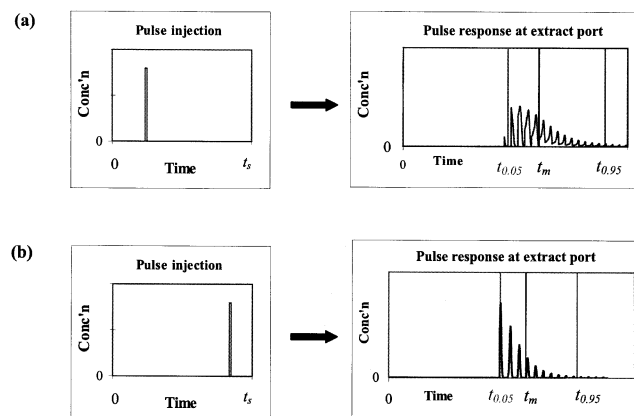


Figure 4. VERSE simulated RTD for a pulse in the extract port of SMB with mass-transfer effects (nonideal system).

(a) Injection of a pulse during the first half of the switching period; (b) injection of a pulse during the second half of the switching period.

Table 1. Comparison of Residence Time in Batch Chromatography and Residence Time in SMB

	Batch Chromatography	SMB
Feed port location	Fixed	Periodically moving
Product ports	One Fixed Downstream from the feed port	Two Periodically moving —Raffinate downstream from feed port (First in, First out) —Extract upstream from feed port (First in, Last out)
Recycle	No	Two recycle streams
Zone flow rate	One	Four
Mean residence time	Migration velocities —Flow rates —Equilibrium constants One column length	Migration velocities —Zone flow rates —Equilibrium constants Four zone lengths Zone configuration Port velocity/recycle ratio
Mechanisms for residence time distribution	Mass transfer	Location of feed and two product ports Periodic port movement Recycle streams/mass transfer
Literature	Plenty	None

similar to that in an ideal system, except that the response peaks are broadened by mass-transfer effects. Table 1 summarizes the fundamental differences in residence time between batch chromatography and SMB.

Mean residence time (t_m), breakthrough time ($t_{0.05}$), and extinction time ($t_{0.95}$)

In this section, the RTD functions proposed in the previous literatures for a batch process (Danckwerts, 1953; Levenspiel, 1972; Fogler, 1986) are introduced to express the RTD in SMB.

A small amount of solute N_0 is injected in a short period of time into an SMB. Effluent history of the solute is then measured at a product port (raffinate or extract port). First, we choose an increment of time Δt which is sufficiently small so that the concentration of solute $C(t)$ exiting between time t and $t + \Delta t$ is essentially constant. The amount of solute molecules ΔN leaving the SMB between time t and $t + \Delta t$ is then

$$\Delta N = C(t) \cdot F_p \cdot \Delta t \quad (1)$$

where F_p is the effluent volumetric flow rate at the product port and ΔN is the amount of solute that has spent an amount of time between t and $t + \Delta t$ inside the SMB. Division of ΔN by the total amount of solute (N_0) that is injected into the SMB gives

$$\frac{\Delta N}{N_0} = \frac{F_p \cdot C(t)}{N_0} \cdot \Delta t \quad (2)$$

Equation 2 represents the fraction of solute molecules that has a residence time in the SMB between t and $t + \Delta t$. The residence time distribution function $E(t)$ is defined as follows (Danckwerts, 1953; Levenspiel, 1972; Fogler, 1986)

$$E(t) = \frac{F_p \cdot C(t)}{N_0} \text{ so that } \frac{\Delta N}{N_0} = E(t) \cdot \Delta t \quad (3)$$

$E(t)$ is the function that describes in a quantitative manner how much time different solute molecules have spent in the SMB. The total amount of solute N_0 is obtained by summing up all solute molecules ΔN between time equal to zero and infinity

$$N_0 = \int_0^\infty F_p \cdot C(t) dt \quad (4)$$

where the effluent volumetric flow rate F_p is kept constant in SMB. Substituting Eq. 4 into Eq. 3, one can express $E(t)$ in terms of effluent history at the product port as follows

$$E(t) = \frac{C(t)}{\int_0^\infty C(t) dt} \quad (5)$$

A majority of the solutes will leave the SMB after spending a period of time in the vicinity of the mean residence time (t_m). Each $E(t)$ curve has its unique mean residence time. Therefore, the small pulses injected at different times have different $E(t)$'s and t_m 's. This indicates that there is a distribution of t_m , which is a function of the injection time. It is inefficient to show all the $E(t)$ curves generated during one switching time. If a distribution curve of t_m is smooth and continuous, it is better to investigate the relationship between injection time and t_m values. This t_m value is the first moment of the $E(t)$ curve

$$t_m = \frac{\int_0^\infty t \cdot E(t) dt}{\int_0^\infty E(t) dt} = \int_0^\infty t \cdot E(t) dt \quad (6)$$

In addition, we are interested in the times that 5% and 95% of the solute molecules leave the SMB ($t_{0.05}$ and $t_{0.95}$, respectively). According to the previous definition of $E(t)$, the $t_{0.05}$ and $t_{0.95}$ can be estimated from the following equations (Levenspiel, 1972; Fogler, 1986)

$$0.05 = \int_0^{t_{0.05}} E(t) dt \quad (7a)$$

$$0.95 = \int_0^{t_{0.95}} E(t) dt \quad (7b)$$

Each $E(t)$ curve generated during one switching time can be well characterized by its t_m , $t_{0.05}$, and $t_{0.95}$. Similarly, the times that 1% and 99% of the solute molecules leave the SMB can also be defined as $t_{0.01}$ and $t_{0.99}$, respectively. These values will be called collectively as the characteristic residence times (CRT), which can be used to analyze the RTD in SMB.

In addition, the standard deviation of each RTD curve can be estimated from the following equation (Levenspiel, 1972; Fogler, 1986)

$$\sigma = \sqrt{\int_0^\infty (t - t_m)^2 \cdot E(t) dt} \quad (8)$$

The magnitude of standard deviation is an indication of the degree of spreading of RTD. The greater the standard deviation, the more spread the distribution curve.

Analysis of residence time in an ideal system: effects of port movement, zone flow rate, and recycle

In this section, the mathematical expression for the residence time of a solute in an ideal system is derived under a given set of operating conditions (four zone flow rates and switching time).

For a linear ideal system, solute velocities in a four-zone SMB can be described by

$$u_{s,i}^j = \frac{u_0^j}{(1 + P \cdot \delta_i)} \quad (9)$$

where i and j stand for component and zone, respectively; u_s is the solute velocity; u_0 is the interstitial velocity; P is the phase ratio, defined as $(1 - \epsilon_b)/\epsilon_b$, and ϵ_b is the interstitial bed voidage; and δ is defined as $Ke\epsilon_p + (1 - Ke\epsilon_p)a$, ϵ_p is the porosity of the particle, and a is the partition coefficient. If the operating conditions are given, the solute velocities in four zones are fixed in the following residence time analysis. In this study, the solute velocities satisfy the following conditions

$$u_{s2}^I - \nu \geq 0 \quad (10a)$$

$$u_{s1}^{II} - \nu \geq 0 \quad (10b)$$

$$u_{s2}^{III} - \nu \leq 0 \quad (10c)$$

$$u_{s1}^{IV} - \nu \leq 0 \quad (10d)$$

where components 1 and 2 indicate a fast-moving solute and a slow-moving solute, respectively, and ν is the average port velocity (= column length / switching time). Equations 10a–10d represent an infinite set of operating parameters (four zone velocities and switching time) that guarantee separation in SMB (Wankat, 1994; Ma and Wang, 1997). Furthermore, Ma and Wang (1997) derived the standing wave equations for systems without mass-transfer effects that give only one set of operating parameters

$$u_0^I = (1 + P\delta_2)\nu \quad (11a)$$

$$u_0^{II} = (1 + P\delta_1)\nu \quad (11b)$$

$$u_0^{III} = (1 + P\delta_2)\nu \quad (11c)$$

$$u_0^{IV} = (1 + P\delta_1)\nu \quad (11d)$$

Based on these conditions (Eqs. 10 and 11), we first investigate the minimum residence time, which is the time required for a solute to reach a product port for the first time. The residence time of the solute recycled back to SMB is also studied. Only the final results are presented here to save space. The detailed derivations are presented in Appendix A. The key equations are discussed below.

For a slow-moving solute (extract product), the minimum residence time (t_{\min}) is calculated from the following equation

$$t_{\min} = (t_s - t_{in}) + t_s \cdot [(N_s^{III} - 1) + N_s^{II}] + t_0^I \quad (12)$$

where t_s is the switching time and t_{in} is the injection time that ranges from 0 to t_s . During initial switching periods, the solute is in either zone II or zone III. As the number of switchings is increased, the amount of time the solute spends in zone III is reduced. N_s^{III} is the smallest number of switchings such that the solute no longer has access to zone III. After the N_s^{III} th switching, the solute migrates in zone II. To enter zone I, additional N_s^{II} switchings are needed. Finally, t_0^I is the amount of time the solute spends in zone I until it exits the extract port. See Appendix A for details in calculating N_s^{III} , and N_s^{II} , and t_0^I .

If the solute is recycled back to zone II, it stays in zone II for a period of $(t_s - t_0^I)$ and moves into zone I after port switching. Compared with the minimum residence time, the residence time of the solute after the n th recycle ($t_{RC,n}$) has additional terms as follows

$$t_{RC,n} \equiv t_{RC,0} + n \cdot t_s + (t_1^I - t_0^I) \cdot \left(\frac{1 - (u_{s2}^{II}/u_{s2}^I)^n}{1 - (u_{s2}^{II}/u_{s2}^I)} \right) \quad (13)$$

where $t_{RC,0} \equiv t_{\min}$ and t_1^I is the amount of time that the solute spends in zone I after the first recycle. The mathematical

expression for t_1^I is also presented in Appendix A. The difference between $t_{RC,n}$ and $t_{RC,n-1}$ reveals an interesting feature of residence time in SMB

$$\lim_{n \rightarrow \infty} [t_{RC,n} - t_{RC,n-1}] = \lim_{n \rightarrow \infty} \left[t_s + (t_1^I - t_0^I) \cdot \left(u_{s2}^{II} / u_{s2}^I \right)^{n-1} \right] = t_s \quad (14)$$

Equation 14 shows that the amount of additional time a recycled solute spends in SMB converges to one switching time after a large number of recycles.

Similarly, the minimum residence time of a fast-moving solute (raffinate product) t_{\min} is calculated from the following equation

$$t_{\min} = (t_s - t_{in}) + t_s \cdot \left[(N_f^{II} - 1) + (N_f^{III} - 1) \right] + t_0^{III} \quad (15)$$

where N_f^{II} is the smallest number of switchings such that the solute can no longer have access to zone II. After the N_f^{II} th switching, the solute migrates in zone III and shifts toward the raffinate port. The solute reaches the raffinate port between the $(N_f^{II} + N_f^{III} - 1)$ th switching and the $(N_f^{II} + N_f^{III})$ th switching. Finally, t_0^{III} is the amount of time the solute spends in zone III after the $(N_f^{II} + N_f^{III} - 1)$ th switching. See Appendix A for details in calculating N_f^{II} , N_f^{III} , and t_0^{III} .

The recycled solute spends a time period of $(t_s - t_0^{III})$ in zone IV and moves into zone III after port switching. The residence time of the solute after the n th recycle ($t_{RC,n}$) is calculated from

$$t_{RC,n} = t_{RC,0} + n \cdot t_s + (t_1^{III} - t_0^{III}) \cdot \left(\frac{1 - (u_{s1}^{IV} / u_{s1}^{III})^n}{1 - (u_{s1}^{IV} / u_{s1}^{III})} \right) \quad (16)$$

where $t_{RC,0} \equiv t_{\min}$ and t_1^{III} is the amount of time that the solute spends in zone III after the first recycle. The mathematical expression for t_1^{III} is also presented in Appendix A.

The resulting Eqs. 12, 13, 15, and 16 show that residence time in SMB is a strong function of injection time, as well as the operating conditions (zone velocities and switching time).

Analysis of characteristic residence times in an ideal system

The results in the previous section can be used to estimate the characteristic residence times (t_m , $t_{0.05}$, and $t_{0.95}$) in a system without mass-transfer effects. The solutes injected at a certain time t^* can have different residence times because of recycle effects. If 40% of the solutes exit the product port and the rest of the solutes remain in the SMB, the shortest residence time (defined as the first residence time) will be the time that 40% of the solutes have spent inside the SMB. If the recycled solutes reach the product port again, 40% of the recycled solutes will also exit the SMB. The time that they have spent inside the SMB will be the second residence time. If we repeat the above procedure, we can find many different residence times for the solutes injected at a certain

time t^* . As a result, there will be a distribution of residence times for the solutes injected at a certain time t^* . The solutes injected at a different time will also have a different residence time distribution. The concept of $E(t)$ mentioned in the previous section can be used to characterize different RTDs resulting from the solutes injected at different times. Either t_m or $t_{0.95}$ can be plotted as a function of injection time. Mathematical description of this approach is presented below.

A small pulse containing an amount of solutes N_0 is injected into SMB at time $t = 0$. First, we define the recycle ratio (rc) as follows

$$rc \equiv \frac{F_r}{F_r + F_p} \quad (17)$$

where F_r and F_p represent the recycled flow rate and product flow rate, respectively, and the recycle ratio rc is the fraction of solutes that is recycled back to SMB. The fraction of solutes that leave SMB is therefore $(1 - rc)$.

Let $t_{RC,i}$ be the residence time of a portion of solutes leaving SMB after the i th recycle. The amount of solute that leaves SMB at time $t = t_{RC,0}$ (or t_{\min}) is $N_0 \cdot (1 - rc)$. Similarly, the amount of solute that leaves SMB at time $t = t_{RC,\infty}$ is $N_0 \cdot (1 - rc) \cdot rc$, and the amount of solute that leaves SMB at time $t = t_{RC,n}$ is $N_0 \cdot (1 - rc) \cdot rc^n$. Finally, the amount of solute that leaves SMB at time $t = t_{RC,\infty}$ is $N_0 \cdot (1 - rc) \cdot rc^\infty$. This is the reason for the formation of a pulse train after t_{\min} , as shown in Figure 2c. For a large recycle ratio, the pulse train decays more slowly. Mass balance is checked by summing up the entire amount of solute from time zero to infinity

$$\begin{aligned} \int_0^\infty C(t) \cdot F_p \cdot dt &= \sum_{i=0}^\infty N_0 \cdot (1 - rc) \cdot rc^i = N_0 \sum_{i=0}^\infty (rc^i - rc^{i+1}) \\ &= N_0 [(1 - rc) + (rc - rc^2) + \dots] = N_0 \quad (18) \end{aligned}$$

Equations 5 and 6 are used to derive the mean residence time (t_m) as follows

$$\begin{aligned} t_m &= \int_0^\infty t \cdot E(t) \cdot dt = \int_0^\infty \frac{t \cdot C(t) \cdot F_p \cdot dt}{\int_0^\infty C(t) \cdot F_p \cdot dt} \\ &= \frac{1}{N_0} \int_0^\infty t \cdot C(t) \cdot F_p \cdot dt = \frac{1}{N_0} \sum_{i=0}^\infty t_{RC,i} \cdot N_0 \cdot (1 - rc) \cdot rc^i \\ &= \sum_{i=0}^\infty t_{RC,i} \cdot (1 - rc) \cdot rc^i \quad (19) \end{aligned}$$

where i is the number of recycles. Substituting Eq. 13 or Eq. 16 into Eq. 19, one can calculate the t_m of the extract or raffinate product with respect to injection time.

In addition, we are interested in $t_{0.95}$, the time that 95% of solutes leave SMB

$$0.95 = \int_0^{t_{0.95}} E(t) \cdot dt = \frac{1}{N_0} \int_0^{t_{0.95}} C(t) \cdot F_p dt$$

$$= \frac{1}{N_0} \sum_{i=0}^{N_R^{0.95}} N_0 \cdot (1 - rc) \cdot rc^i = 1 - rc^{N_R^{0.95} + 1} \quad (20)$$

Solving Eq. 20 for $N_R^{0.95}$ gives

$$N_R^{0.95} = \frac{\log(0.05)}{\log(rc)} - 1 \quad (21)$$

where $N_R^{0.95}$ implies the number of recycles such that 95% of the solutes leave SMB. The value of $N_R^{0.95}$ should be an integer; otherwise, the integer closest to $N_R^{0.95}$ will be chosen. Plugging the resulting value of $N_R^{0.95}$ into Eqs. 13 or 16, one can obtain the $t_{0.95}$ of extract or raffinate product. It is straightforward from Eq. 21 that a higher recycle ratio always increases $N_R^{0.95}$, resulting in a larger $t_{0.95}$.

Similarly, we can also estimate the number of recycles corresponding to $t_{0.01}$ and $t_{0.05}$, but it is available only when the recycle ratio is greater than 0.99 and 0.95, respectively. If $t_{0.95}$ is replaced by $t_{0.99}$ in Eq. 20, it gives the number of recycles required for 99% of solutes to leave SMB.

Effect of selectivity on residence time

Selectivity is defined here as the ratio between the migration speed of fast-moving solute and that of slow-moving solute as follows

$$\text{Selectivity} = (1 + P\delta_2)/(1 + P\delta_1) \quad (22)$$

If the determination of zone interstitial velocities is based on the standing wave equations (Eqs. 11a–11d), a different selectivity results in different zone interstitial velocities and different residence times.

Since a fast-moving solute travels from the feed port to the raffinate port, the residence time of a fast-moving solute is largely dependent on the difference between its linear velocity in zone III and the average port velocity (ν). The net linear velocity of a fast-moving solute in zone III $u_{w,1}^{III}$ is given by

$$u_{w,1}^{III} \equiv u_{s,1}^{III} - \nu = \frac{u_0^{III}}{(1 + P \cdot \delta_1)} - \nu \quad (23)$$

Substitution of Eqs. 11c and 22 into Eq. 23 gives

$$u_{w,1}^{III} = (\text{Selectivity} - 1) \cdot \nu \quad (24)$$

Equation 24 reveals that a lower selectivity decreases $u_{w,1}^{III}$ resulting in a longer residence time of a fast-moving solute. Similarly, the net linear velocity of a slow-moving solute in zone II can also be expressed as a function of selectivity as

follows

$$|u_{w,2}^{II}| \equiv |u_{s,2}^{II} - \nu| = \left(1 - \frac{1}{\text{Selectivity}}\right) \cdot \nu \quad (25)$$

where the $u_{w,2}^{II}$ has a negative value. Like a fast-moving solute, a slow-moving solute also has a longer residence time as selectivity decreases (Eq. 25).

Selectivity affects the recycle ratio, which has a large impact on the magnitude of the characteristic residence times (CRT). Equations 11 and 22 can be used to derive the relationship between recycle ratio and selectivity as follows

$$\text{Recycle ratio at extract port} = \frac{F(II)}{F(II) + F_{\text{ext}}} = \frac{u_0^{II}}{u_0^I}$$

$$= \frac{(1 + P \cdot \delta_1)}{(1 + P \cdot \delta_2)} = \frac{1}{\text{Selectivity}} \quad (26)$$

$$\text{Recycle ratio at raffinate port} = \frac{F(IV)}{F(IV) + F_{\text{raf}}} = \frac{u_0^{IV}}{u_0^{III}}$$

$$= \frac{(1 + P \cdot \delta_1)}{(1 + P \cdot \delta_2)} = \frac{1}{\text{Selectivity}} \quad (27)$$

As shown in Eqs. 26 and 27, a lower selectivity requires a higher recycle ratio to achieve the four standing waves, and, therefore, longer residence times.

In Eq. 10, the equality conditions correspond to the standing wave conditions where the recycle ratio for each exit port is fixed. In contrast, the inequality conditions in Eq. 10 can allow a smaller recycle ratio to reduce the residence time of a solute. The inequality conditions include the pinched wave design operating conditions, which will be proposed as one of the ways to reduce the solute residence time in the section of results and discussion.

Analysis of residence time in a nonideal system using rate model simulations — effects of mass transfer

Simulations based on a detailed rate model (VERSE) are used to take into account mass-transfer effects in the analysis of residence time in SMB. In this analysis, effluent history is first generated from the rate model simulations, and used to estimate the CRT (t_m , $t_{0.05}$, and $t_{0.95}$) in SMB.

The rate model consists of mass balance equations for both mobile and stationary phases. The model equations consider convection, axial dispersion, film mass transfer, and intra-particle diffusion. To solve the model equations for effluent history, the method of orthogonal collocation on finite elements (Villadsen and Michelsen, 1978; Finlayson, 1980; Baker, 1983) is applied. The partial differential equations in the model are converted to ordinary differential equations (ODEs) through polynomial approximations of the spatial partial derivatives; Legendre polynomials are used in the axial direction and Jacobi polynomials are used in the particle radial direction (Berninger et al., 1991). DASSL (Petzold, 1982), a differential/algebraic system solver, is used to inte-

Table 2. Intrinsic Parameter Values Used in the Standing Wave Design

	HPI	Insulin	ZnCl ₂
<i>Ke</i>	0.19	0.74	0.99
<i>D_∞</i> [m ² /s]	8.00 × 10 ⁻¹¹	9.15 × 10 ⁻¹¹	6.60 × 10 ⁻¹⁰
<i>D_p</i> [m ² /s]	3.33 × 10 ⁻¹¹	3.82 × 10 ⁻¹¹	2.75 × 10 ⁻¹⁰
<i>k_f</i> [m/s]	The Wilson and Geankoplis (1966) correlation The Chung and Wen (1968) correlation*		
<i>E_b</i> [m ² /s]			
Column properties	<i>ε_b</i> = 0.35, <i>ε_p</i> = 0.89		

*The *E_b* value of insulin in zone III of Ring I is chosen to be 40 times as large as that estimated from the Chung and Wen (1968) correlation.

grate the ODEs in the time domain. All of these numerical computations are carried out in a VERSE simulator, which has been validated in several previous studies (Whitley, 1990; Berninger et al., 1991; Ma et al., 1996; Hritzko, 2001; Xie et al., 2002).

In order to account for axial dispersion and delay in the dead volume, the dead volume was considered as a continuously stirred tank (CST) between two connected columns. The general equation for the CST is given by

$$DV \frac{dC_{\text{out}}}{dt} = F(C_{\text{in}} - C_{\text{out}}) \quad (28)$$

where *DV* is the dead volume, *F* is the volumetric flow rate, *C_{in}* is the concentration at the CST inlet, and *C_{out}* is the concentration at the CST outlet.

Parameters

The results of the RTD for the solutes injected during one switching period are sufficient to show the representative behavior because the residence time history is repeated in every switching time in a linear isotherm system. The operating conditions of the tandem SMB were determined from the standing wave design (Ma and Wang, 1997; Hritzko et al., 2002) for nonideal systems. The effect of dead volume on RT and RTD is also investigated. The intrinsic parameters used in the standing wave design have been reported by Xie et al. (2002) and are listed in Table 2. Note that in the standing wave design equations, the *E_b* value of insulin in zone III of Ring I is chosen to be 40 times as large as that estimated from the Chung and Wen (1968) correlation. This is to over-

come the large dispersion of insulin in zone III due to non-ideal flow or other mechanisms (Xie et al., 2002). The resulting zone flow rates and switching time (*t_s*) for Ring I and Ring II are listed in Table 3 and will be used in the RTD analysis. For Ring II, two sets of operating conditions were determined for two different zone configurations. Unless noted otherwise, Ring II has the operating conditions based on the zone configuration 2-3-3-2.

Results and Discussion

First, the local equilibrium analysis (LEA) is validated using rate model simulations. The assumption that RTD is independent of pulse concentration is also validated using the simulations. The LEA is used to investigate the effects of port location, port movement, recycle, and zone flow rates on the residence time of insulin in an ideal system. The results from the LEA are compared with those from rate model simulations in order to isolate the effects of injection time and recycle ratio from the effects of mass transfer. The effects of dead volume, selectivity, zone lengths, and zone flow rates on the residence time are also studied. Finally, strategies to shorten the residence time in SMB are formulated and validated with rate model simulations.

Comparison of CRT from LEA and VERSE simulations

In this study, the LEA is used to understand the effects of port movement and recycle on the residence time of insulin in an ideal system. To validate the LEA used in the RTD analysis, the results from the LEA were compared with those from VERSE simulations for Ring I with significantly re-

Table 3. Operating Conditions of a Tandem SMB Used in the Analysis of RTD

		Ring I	Ring II	
Zone Configuration*		2-2-4-2	2-3-3-2	2-2-2-2
Zone linear velocities** [m/s]	Zone I	1.878 × 10 ⁻⁴	1.829 × 10 ⁻⁴	1.905 × 10 ⁻⁴
	Zone II	1.101 × 10 ⁻⁴	1.550 × 10 ⁻⁴	1.622 × 10 ⁻⁴
	Zone III	1.655 × 10 ⁻⁴	1.815 × 10 ⁻⁴	1.888 × 10 ⁻⁴
	Zone IV	1.085 × 10 ⁻⁴	1.513 × 10 ⁻⁴	1.576 × 10 ⁻⁴
Inlet and outlet linear velocities** [m/s]	Feed	5.540 × 10 ⁻⁵	2.652 × 10 ⁻⁵	2.652 × 10 ⁻⁵
	Desorbent	7.930 × 10 ⁻⁵	3.153 × 10 ⁻⁵	3.290 × 10 ⁻⁵
	Raffinate	5.708 × 10 ⁻⁵	3.017 × 10 ⁻⁵	3.117 × 10 ⁻⁵
	Extract	7.762 × 10 ⁻⁵	2.788 × 10 ⁻⁵	2.825 × 10 ⁻⁵
Switching time [s]		1.804 × 10 ³	2.172 × 10 ³	2.086 × 10 ³

*Single column length = 0.15 m.

***u₀* = *F*/*(ε_bS)*, where *F* and *S* are the flow rate and the column cross-sectional area, respectively.

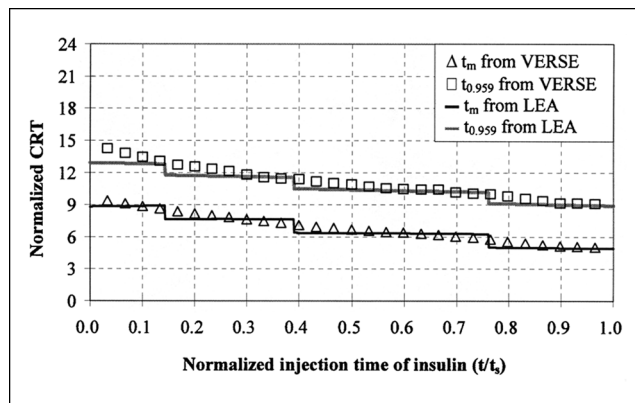


Figure 5. Comparison of the characteristic residence times of insulin in Ring I from VERSE simulations and the LEA with recycle effects.

The axial dispersion coefficient of insulin was decreased by 90%.

duced mass-transfer effects. As mass-transfer effects are reduced, the results from VERSE simulations should approach the results from the LEA. As a result of the large dispersion in the first ring, axial dispersion is the dominant (95%) mass-transfer mechanism. For this reason, we reduced the axial dispersion parameter by 90% in the simulation so that we can compare the RTD results obtained from the simulation with those from the LEA. As shown in Figure 5, the t_m and $t_{0.959}$ values obtained from simulations are in close agreement with the values obtained from the LEA with recycle effects.

Confirmation of the independence of RTD results on pulse size and pulse concentration

In this study, the RTD analysis in SMB is based on the injection of small pulses. It is necessary to check if the results are independent of pulse size. This investigation was carried out using VERSE. First, one large pulse of 3 min was injected into Ring I SMB. Secondly, the large pulse was divided into three small pulses, which were then injected in succession. The effluent histories from the two different input modes are in perfect agreement, indicating that the results on RTD are general and independent of pulse size. Furthermore, the pulse concentration should not affect the results. The lack of dependence of RTD on the pulse concentration is also confirmed by VERSE simulations. Two small pulses of insulin with different concentrations are injected into Ring I SMB. The two effluent histories are identical, indicating that the results on RTD are independent of feed concentration for linear isotherm systems.

Effects of port location and port movement shown by the local equilibrium analysis

In a four-zone SMB, the raffinate port is located downstream from the feed port, whereas the extract port is located upstream from the feed port. The earlier the fast-moving solute is injected during the switching period, the earlier it exits the raffinate port, or first in, first out (Figure 3b). In

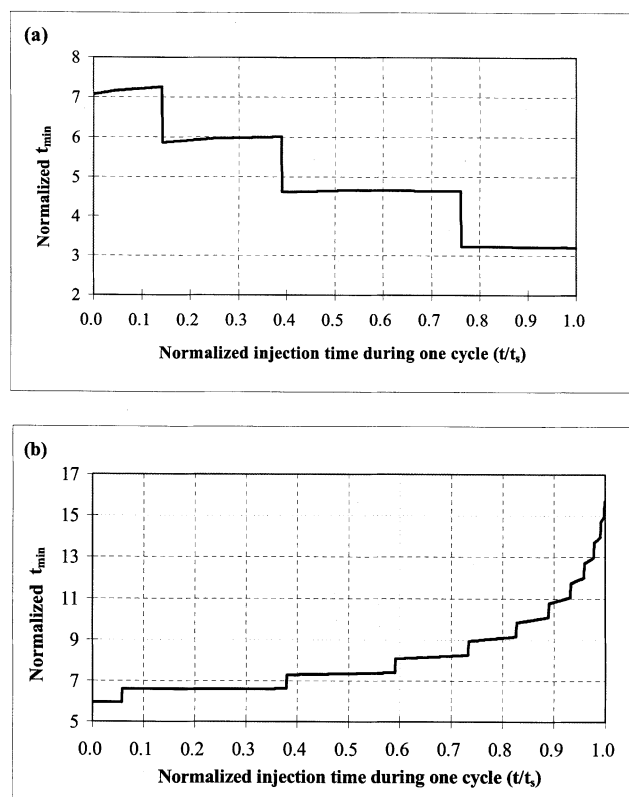


Figure 6. Normalized t_{min} as a function of injection time based on the LEA without recycle effects in Ring I ($t_s = 1804$ s).

(a) Insulin (extract product); (b) HPI (raffinate product). See Figure 3 for details in the occurrence of several distinct groups in t_{min} .

contrast, the earlier the slow-moving solute is injected during the switching period, the later it exits the extract port, or first in, last out (Figure 3a).

We examine first the time required for a solute to reach the product port for the first time, which is defined here as the minimum residence time (t_{min}). This does not include any mass-transfer or recycle effects. Therefore, it shows only the effects of injection time, port location, port movement, and zone flow rates on the minimum residence time. The t_{min} for each injection time during one switching period is calculated from Eq. 12 or 15. The results are shown in Figures 6 and 7 where the t_{min} and the injection time are normalized by the switching time. As shown in these figures, solutes injected at different times have different t_{min} 's. As expected from Eqs. 12 and 15, there is a distribution of t_{min} according to the solute injection time.

In Ring I, insulin is the slow moving solute and the extract product. The insulin injected at the beginning of a switching period has the largest t_{min} (Figure 6a). In contrast, the HPI (the fast moving solute or the raffinate product) injected at the beginning of the switching period has the smallest t_{min} (Figure 6b). Notice that the t_{min} for the raffinate product increases significantly toward the end of the injection period. This is caused by the low flow rate and the large length in zone III.

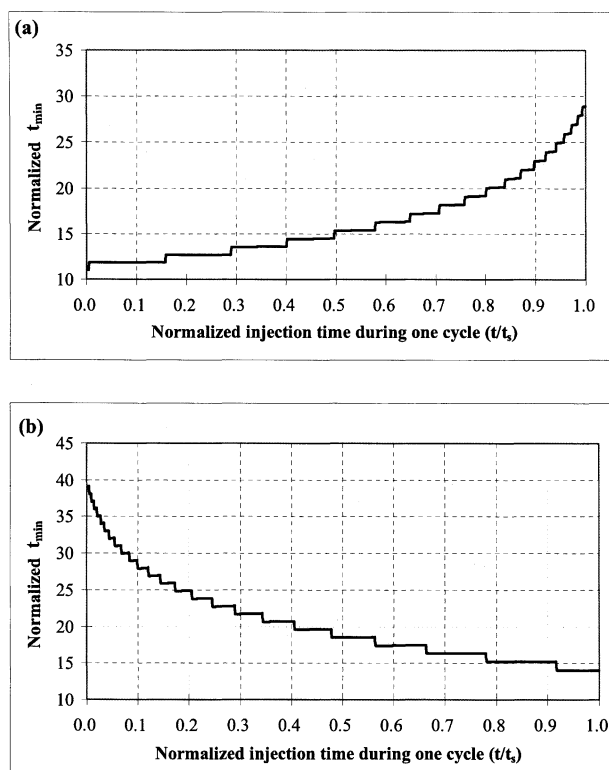


Figure 7. Normalized t_{\min} as a function of injection time based on the LEA without recycle effects in Ring II ($t_s = 2172$ s).
(a) Insulin (raffinate product); (b) ZnCl_2 (extract product).

Several bumps are observed in the distribution curve of t_{\min} in Figure 6. These “bumps” are related to a sharp change in the solute residence time due to port movement. As shown in Figure 3, the traveling distances of the solutes injected at different times are classified into several groups. In each group, there is little difference in the traveling distance before exiting the product port. Between two adjacent groups, the traveling distance differs by one column length because of port movement. This behavior causes the “bumps” in the distribution curve of t_{\min} in Figure 6.

In Ring II, insulin is the fast-moving solute and the raffinate product. Thus, the t_{\min} distribution of insulin in Ring II (Figure 7a) has a trend opposite to that in Ring I, where insulin is the slow-moving solute. Figure 7b shows the t_{\min} distribution of ZnCl_2 , which is the extract product in Ring II. As expected, the ZnCl_2 injected at the beginning of the switching period has the largest t_{\min} (or first in, last out).

Recycle effects shown by the local equilibrium analysis

The recycle effects are analyzed first for an ideal system. The mean residence time t_m is calculated as follows. Equation 17 is used to calculate the recycle ratio (rc). Equations 13 and 16 are used to find the residence time with recycle effects ($t_{RC,n}$), which are then used in Eq. 19 to find t_m . The estimation of t_m needs an infinite number of recycles according to Eq. 19, but 100 recycles are sufficient because there is almost no change in the t_m value beyond one hundred recy-

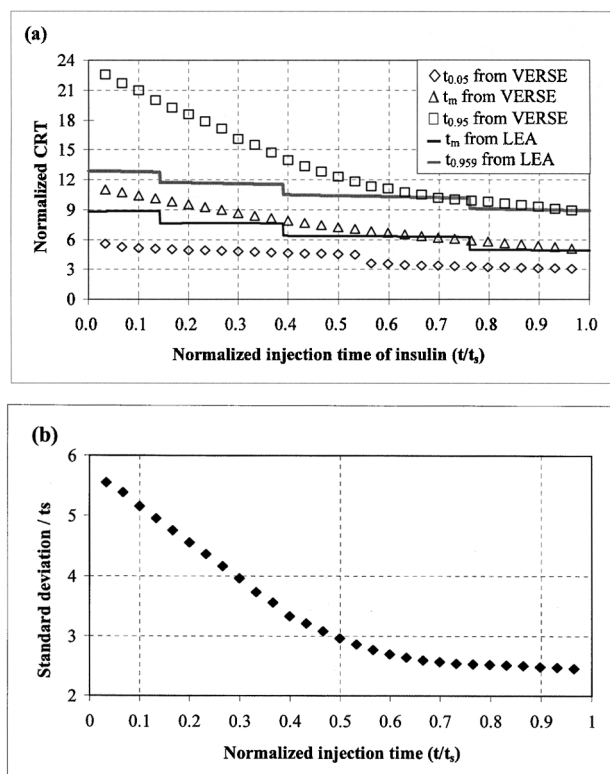


Figure 8. Analysis of the residence time of insulin (extract product) in Ring I.

(a) Normalized characteristic residence times of insulin; (b) normalized standard deviation of each $E(t)$ curve with respect to injection time (based on VERSE simulations).

cles. The value of $N_R^{0.95}$ is determined from Eq. 21 and used to estimate $t_{0.95}$. Note for this example, $t_{0.05}$ does not exist for Ring I or Ring II because, at the minimum residence time, 41% of insulin exit Ring I (for a recycle ratio of 0.59) and 17% of insulin exit Ring II (for a recycle ratio of 0.83).

The resulting CRT of insulin for Ring I are presented in Figure 8a. We see that the overall trend of CRT in Figure 8a is similar to that of the t_{\min} distribution shown in Figure 6a. The recycle of insulin causes an additional increase in its residence time and smoothes out the “bumps” explained in the previous section. The same conclusion is also reached in Ring II by comparing Figure 9a with Figure 7a.

Mass-transfer effects shown by VERSE simulations

The distributions of t_m and $t_{0.95}$ obtained from the equilibrium analysis include recycle effects. They can be compared with those obtained from the rate model simulations to show any mass-transfer effects. VERSE simulations were used to obtain the solutions for 29 small tracer pulses of insulin injected within one switching period in Ring I and 35 small pulses in Ring II. The size of each pulse was sufficiently small (0.01 min) to have its unique injection time. The spreading and the tailing of each tracer pulse are due to both mass-transfer effects and recycle effects, resulting in a residence time distribution curve for each pulse injected at a given time. The CRT were calculated from Eqs. 6 to 7b and the standard

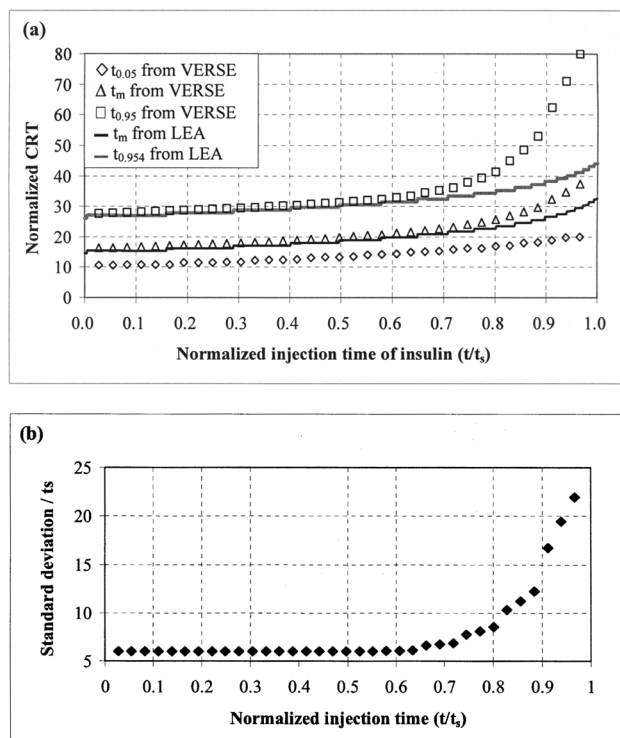


Figure 9. Analysis of the residence time of insulin (raffinate product) in Ring II.

(a) Normalized characteristic residence times of insulin; (b) normalized standard deviation of each $E(t)$ curve with respect to injection time (based on VERSE simulations).

deviation of each RTD curve was calculated from Eq. 8. The results are shown as a function of injection time in Figure 8 for Ring I and Figure 9 for Ring II.

The differences between the results from VERSE simulations and those from the LEA with recycle effects are due to mass-transfer effects, which broaden the RTD and increase all characteristic residence times. The differences are larger for the first half switching period in Ring I (Figure 8a) because the pulses injected earlier exit the extract port later, and they are spread out more by mass-transfer effects.

In Figure 8a, there is a “bump” at $t/t_s = 0.55$ in the $t_{0.05}$ data. This “bump” in Figure 8a is related to the multiple “bumps” in the results obtained from the equilibrium analysis (Figure 6a). Mass-transfer effects spread out the bumps and make the small bumps at small injection time ($t/t_s = 0.14$) disappear. The spreading of the bump at $t/t_s = 0.39$ and that at $t/t_s = 0.76$ give an apparent bump at $t/t_s = 0.55$ in the $t_{0.05}$ data in Figure 8a.

Effects of selectivity and zone length

The results in Figure 9a show that the residence times of insulin in Ring II are much longer than those in Ring I (Figure 8a). This is due to the differences in selectivity and zone length (or zone configuration) between the two rings. As calculated from the intrinsic parameter values in Table 2, the selectivity between insulin and HPI for the separation in Ring I is 1.7 and the selectivity between ZnCl_2 and insulin for the separation in Ring II is 1.2. As expected from Eqs. 26 and 27, the lower selectivity for Ring II leads to a higher recycle ratio (Table 4) and longer residence times as explained below.

For Ring II, a specific set of linear velocities from the standing wave design are chosen such that the adsorption wave of the slow moving solute (ZnCl_2) is standing in zone III. Therefore, the migration velocity of ZnCl_2 in zone III equals the average port velocity (v). Because of the small selectivity between ZnCl_2 and insulin, the migration velocity of insulin is similar to the port velocity. This in turn leads to a long residence time of insulin in Ring II.

Furthermore, there are three columns between the feed port and the product (raffinate) port in Ring II, but only two columns between the feed port and the extract port in Ring I. This means that insulin needs to travel a longer distance in Ring II than in Ring I. This also contributes to a longer residence time in Ring II.

Effect of dead volume on residence time

As is often the case, SMB unit has a certain amount of dead volume due to valves and tubing between each column. This extra-column dead volume causes additional wave spreading and an apparent increase in residence time as solutes migrate from one column to the next. This is why the

Table 4. Input Data for the LEA with Recycle Effects in Ring I and Ring II

	$\frac{F_r}{\epsilon_b S}$ [m/s]	$\frac{F_p}{\epsilon_b S}$ [m/s]	rc	N_R
Ring I	1.101×10^{-4}	7.762×10^{-5}	0.587	5*
Ring II	1.513×10^{-4}	3.017×10^{-5}	0.834	16**

*After the 5th recycle, 95.9% of solutes leave SMB.

**After the 16th recycle, 95.4% of solutes leave SMB.

Table 5. Operating Conditions of Ring I with Dead Volume (3% of the Bed Volume)

Zone linear velocities [m/s]	Zone I	Zone II	Zone III	Zone IV	Inlet and outlet linear velocities [m/s]	Feed	Desorbent	Raffinate	Extract

*Switching time (t_s) = 1.768×10^3 s.

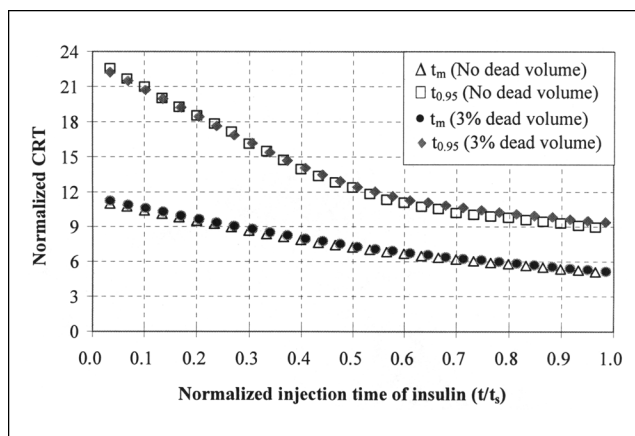


Figure 10. Effect of dead volume on the characteristic residence times of insulin in Ring I.

All the data were obtained from VERSE simulations.

standing wave design uses an apparent retention factor δ^* to account for the delay (Xie et al., 2002). It is expected that the dead volume will have little effect on residence time if the dead volume is relatively small compared to the column volume. To test this hypothesis, VERSE simulations were performed for the case where the extra-column dead volume in Ring I is 3% of the bed volume. The operating conditions used in the simulations are listed in Table 5. The operating conditions in Table 5 take into account the effect of dead volume and, thus, are different from the operating conditions in Table 3, which are based on negligible dead volume. Figure 10 shows that the differences in the CRT of insulin in Ring I from the two different operating conditions are small.

Effect of the flow rates in zone II and zone III on residence time shown by the equilibrium analysis

In the standing wave design, the flow rates in the four zones are chosen so that the four waves are standing in the appropriate zones in a time-averaged sense (Figures 11a and 11c). In this case, the velocities of the fast-moving solute in zone II and the slow moving solute in zone III relative to the port velocity are minimized to achieve the maximum throughput. However, this leads to large residence times of both solutes.

One can modify the zone flow rates from the standing wave design to shorten the residence time of either the fast moving solute or the slow moving solute without any loss in purity and yield. In this case, one can increase the zone II flow rate such that the trailing wave of the fast-moving solute in zone II migrates faster than the port and reach the raffinate sooner (Figure 11b). One can also decrease the zone III flow rate such that the advancing wave of the slow-moving solute in zone III migrates slower than the port and reach the extract port sooner (Figure 11d). These waves are no longer “standing” but “stuck” or “pinched” between zone II and zone III as shown in Figures 11b and 11d. These waves have been defined previously as the “pinched waves” (Hritzko et al., 2002).

First, the equilibrium analysis was used to show the effect of the pinched wave design on the residence time of insulin (fast-moving solute) in Ring II. In order to pinch the trailing

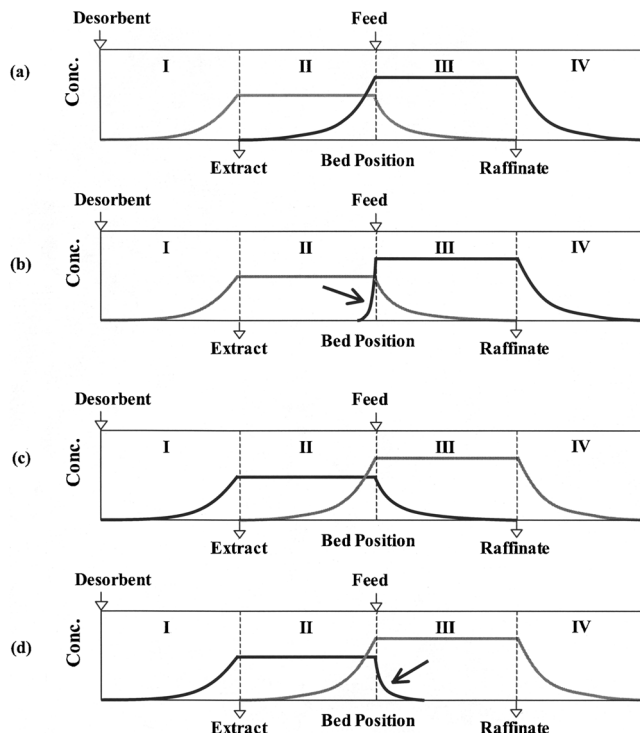


Figure 11. Comparison of the column profiles from the standing wave design and the pinched wave design.

(a) Standing wave design (product = fast-moving solute); (b) pinched wave design (product = fast-moving solute); (c) standing wave design (product = slow-moving solute); (d) pinched wave design (product = slow-moving solute).

wave of insulin, the zone II flow rate was increased. Figure 12a shows the effect of increasing zone II flow rate on the t_{\min} of insulin. One can see that the t_{\min} of insulin is significantly reduced by increasing zone II flow rate, especially for insulin injected towards the end of a switching period.

The effectiveness of the pinched wave design on the residence time of ZnCl_2 (slow-moving solute) was also investigated. Figure 12b shows the effect of decreasing zone III flow rate on the t_{\min} of ZnCl_2 . Since ZnCl_2 needs to exit the extract port, a lower zone III flow rate results in a smaller t_{\min} of ZnCl_2 as shown in Figure 12b.

The results in this section show that one can shorten the residence time of one key component by using the “pinched” wave designs, in which either the trailing wave of the fast solute or the advancing wave of the slow solute is pinched between zone II and zone III. This result will be confirmed by VERSE simulations in the next section.

Strategies to reduce the residence time of insulin

According to the equilibrium analysis, the residence time of insulin in SMB is a strong function of the injection time. This trend was even greater when mass-transfer effects were taken into account. There is a general concern that insulin molecules spending much longer than 30 h in the mobile phase can undergo aggregation or denaturation. The first effective strategy will be to inject the feed during only part of

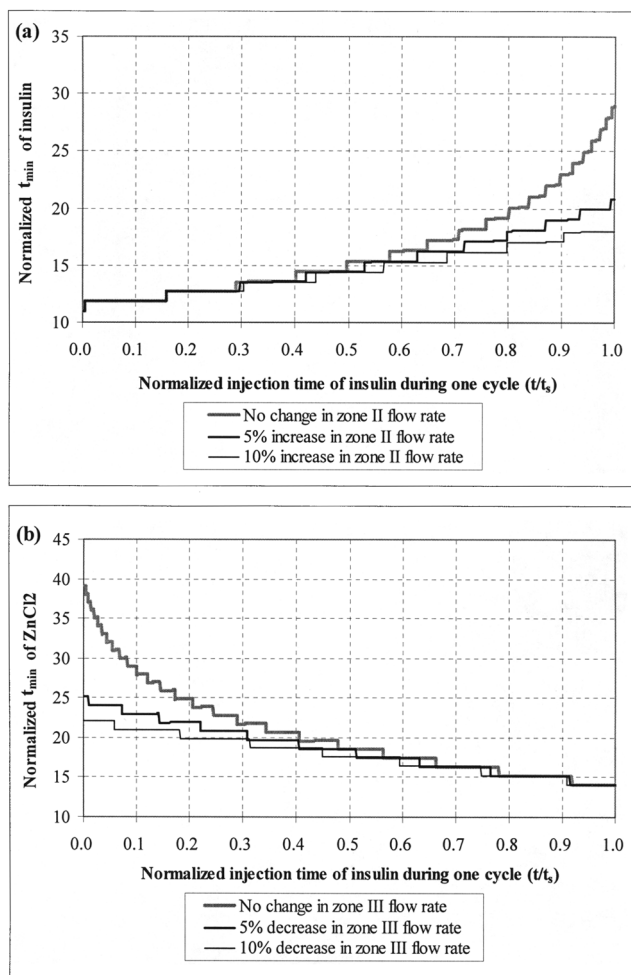


Figure 12. Effect of zone flow rates on the t_{\min} of insulin and $ZnCl_2$ in Ring II (pinched wave design).

Feed flow rate is adjusted according to the variation of zone II or zone III flow rate. (a) Insulin (fast-moving solute); (b) $ZnCl_2$ (slow-moving solute).

the switching time. Our analysis suggests that the insulin molecules injected during the second half-switching time have a shorter residence time in Ring I (Figure 8a), and a longer residence time in Ring II (Figure 9a). Therefore, in order to shorten the residence time of insulin, the feed should be injected only during the second half-switching time in Ring I, and during the first half-switching time in Ring II. During the rest of the switching time, the desorbent should be injected in order to maintain constant zone flow rates. VERSE simulation results based on the partial feeding strategy are shown in Figure 13. One can see that the insulin injected based on the partial feeding strategy exits earlier, resulting in a shorter residence time.

A second strategy is to use the pinched wave design where the flow rate in either zone II or zone III is modified. The equilibrium analysis shows that reducing the flow rate in zone III shortens the residence time of the slow moving solute (or the extract product), whereas increasing the flow rate in zone II shortens the residence time of the fast moving solute (or

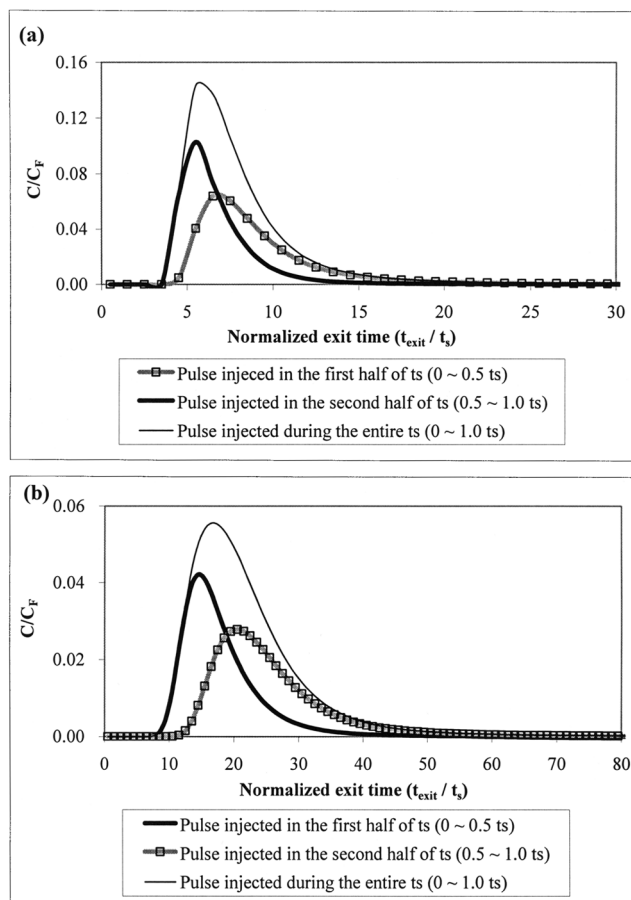


Figure 13. Effect of partial feeding on the residence time of insulin.

(a) Effluent history of insulin (extract product) in Ring I from VERSE simulations; (b) effluent history of insulin (raffinate product) in Ring II from VERSE simulations. Concentrations in the effluent histories are averaged over one switching period.

the raffinate product) (Figures 11 and 12). Both cases can shorten the residence time, but throughput is decreased accordingly. This strategy was applied to reduce the residence time of insulin in Ring II. All the operating conditions remained unchanged except the flow rates of zone II and feed. In order to compare this strategy with the partial feeding strategy, the zone II flow rate was increased such that throughput was 50% of that of the standing wave design. For this case, both VERSE simulations and LEA with recycle effects were used to find the residence time of insulin. As shown in Figure 14a, the residence time and RTD of insulin are significantly shortened compared to those from the standing wave design and full feeding (Figure 9a). In addition, the results from VERSE are close to those from the LEA with recycle effects over the full switching period (Figure 14a), indicating that the effects of mass transfer on RTD are significantly reduced in the "pinched" wave design operating conditions. The effluent histories of insulin in Ring II show that insulin leaves SMB earlier if the operating conditions are based on the "pinched" wave design (Figure 14b). The LEA with recycle effects was used to investigate the effect of decreasing throughput on the mean residence time. Since t_m is

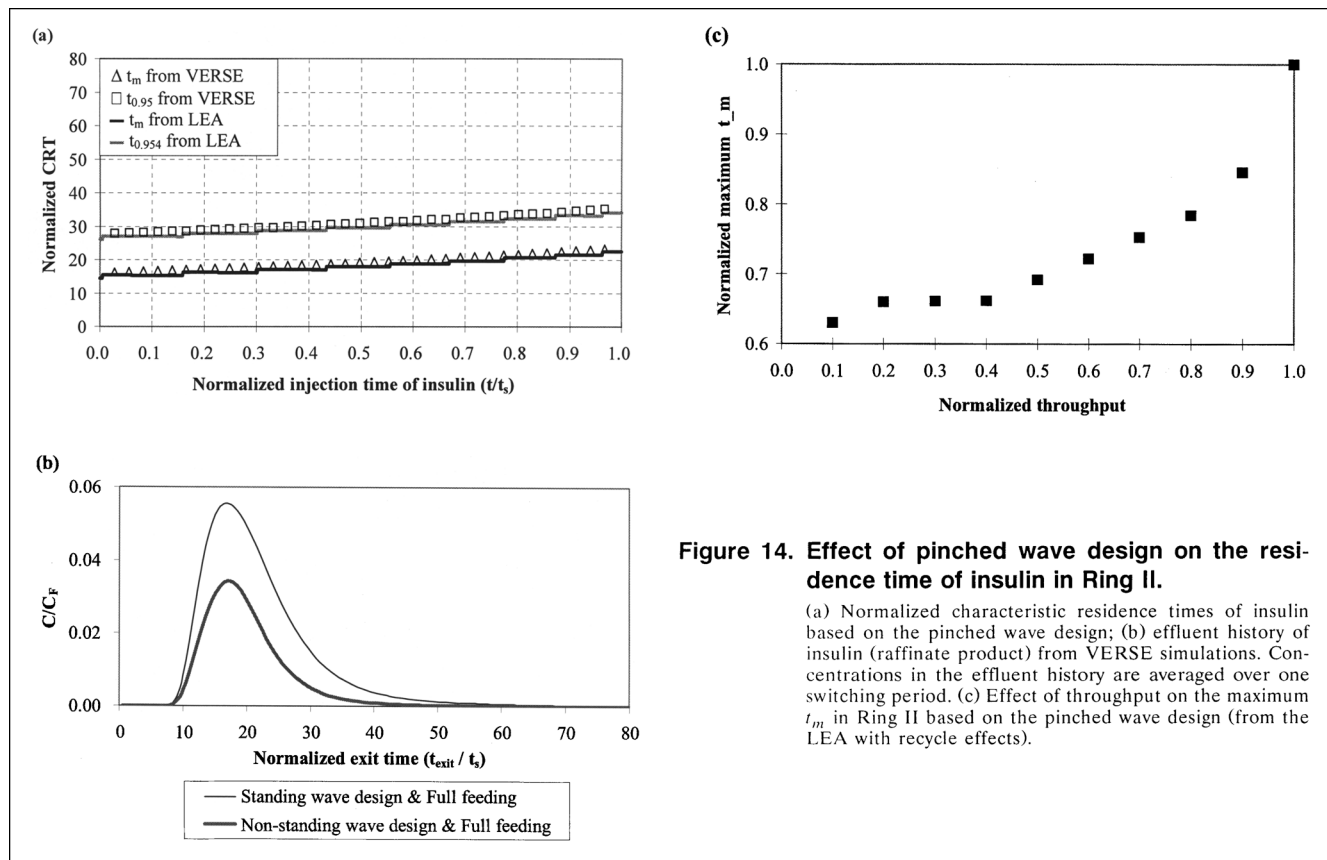


Figure 14. Effect of pinched wave design on the residence time of insulin in Ring II.

(a) Normalized characteristic residence times of insulin based on the pinched wave design; (b) effluent history of insulin (raffinate product) from VERSE simulations. Concentrations in the effluent history are averaged over one switching period. (c) Effect of throughput on the maximum t_m in Ring II based on the pinched wave design (from the LEA with recycle effects).

a function of injection time, the maximum value of t_m for each case is shown in Figure 14c. Decreasing the throughput to below 50% does not help reduce the residence time.

Table 6 compares the standing wave design with the two strategies (partial feeding strategy and pinched wave design) in terms of t_m , $t_{0.95}$, and $t_{0.99}$ for the feed pulse injected dur-

ing one switching period. As expected, the two strategies result in a smaller t_m , $t_{0.95}$, and $t_{0.99}$ than those of the standing wave design. Note that the differences in $t_{0.99}$ are much larger than the differences in t_m or $t_{0.95}$. This is due to a substantial reduction in the degree of tailing from the two strategies. Between the two strategies, the partial feeding strategy ap-

Table 6. Residence Times of Insulin in Ring I and Ring II from the Standing Wave Design, Partial Feeding Strategy, and Pinched Wave Design

		Ring I	Ring II
Standing wave design (100% throughput)	$t_{0.01}$	7.272×10^3 s ($4.03 t_s$)	2.344×10^4 s ($10.8 t_s$)
	$t_{0.05}$	7.416×10^3 s ($4.11 t_s$)	2.718×10^4 s ($12.5 t_s$)
	t_m	1.501×10^4 s ($8.32 t_s$)	4.932×10^4 s ($22.7 t_s$)
	$t_{0.95}$	2.844×10^4 s ($15.8 t_s$)	8.928×10^4 s ($41.1 t_s$)
	$t_{0.99}$	5.292×10^4 s ($29.3 t_s$)	1.631×10^5 s ($75.1 t_s$)
Partial feeding strategy (50% throughput)	$t_{0.01}$	7.236×10^3 s ($4.01 t_s$)	2.160×10^4 s ($9.94 t_s$)
	$t_{0.05}$	7.344×10^3 s ($4.07 t_s$)	2.538×10^4 s ($11.7 t_s$)
	t_m	1.256×10^4 s ($6.97 t_s$)	3.996×10^4 s ($18.4 t_s$)
	$t_{0.95}$	2.052×10^4 s ($11.3 t_s$)	6.624×10^4 s ($30.5 t_s$)
	$t_{0.99}$	3.744×10^4 s ($20.8 t_s$)	1.051×10^5 s ($48.4 t_s$)
Pinched wave design (50% throughput)	$t_{0.01}$	7.272×10^3 s ($4.03 t_s$)	2.336×10^4 s ($10.8 t_s$)
	$t_{0.05}$	7.380×10^3 s ($4.09 t_s$)	2.606×10^4 s ($12.0 t_s$)
	t_m	1.307×10^4 s ($7.25 t_s$)	4.428×10^4 s ($20.4 t_s$)
	$t_{0.95}$	2.124×10^4 s ($11.8 t_s$)	7.200×10^4 s ($33.1 t_s$)
	$t_{0.99}$	3.744×10^4 s ($20.8 t_s$)	1.123×10^5 s ($51.7 t_s$)

* t_s of Ring I: 1.804×10^3 s; t_s of Ring II: 2.172×10^3 s.

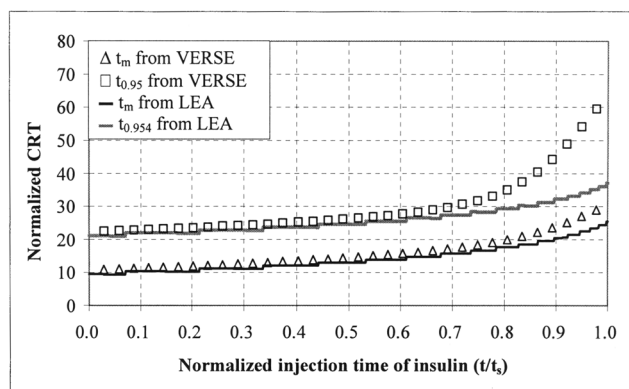


Figure 15. Normalized characteristic residence times of insulin in Ring II based on shorter zone lengths (2-2-2-2 zone configuration).

pears to shorten the residence time slightly more than the pinched wave design.

Decreasing zone length can also shorten residence time. To confirm this strategy, we investigated the residence time in Ring II with shorter lengths in zone II and zone III (2-2-2-2 zone configuration). New operating conditions were determined from the standing wave design and are listed in Table 3. Figure 15 shows the resulting t_m and $t_{0.95}$ from VERSE simulations and LEA with recycle effects. A comparison of Figures 9a and 15 reveals that the decrease of zone lengths helps shorten the residence time of insulin. However, mass-transfer effects are still pronounced in the second half-switching period regardless of zone length. For this reason, only a decrease in zone length may be effective in reducing t_m but not in reducing $t_{0.95}$, which is largely affected by the degrees of spreading and tailing. As listed in Tables 6 and 7, Ring II with shorter zone lengths based on the standing wave design has a smaller t_m , but a larger $t_{0.95}$ than those with standard zone lengths based on the partial feeding strategy or the pinched wave design.

Both partial feeding strategy and pinched wave design can also be applied to the Ring II with shorter zone lengths (2-2-2-2 zone configuration). As listed in Table 7, the residence time of insulin is greatly shortened when either partial feeding strategy or pinched wave design is used together with shorter zone lengths. Both strategies plus shorter zone lengths can reduce the insulin residence time $t_{0.95}$ from 45 h to less than 30 h (Table 7). In order to compare all the strategies,

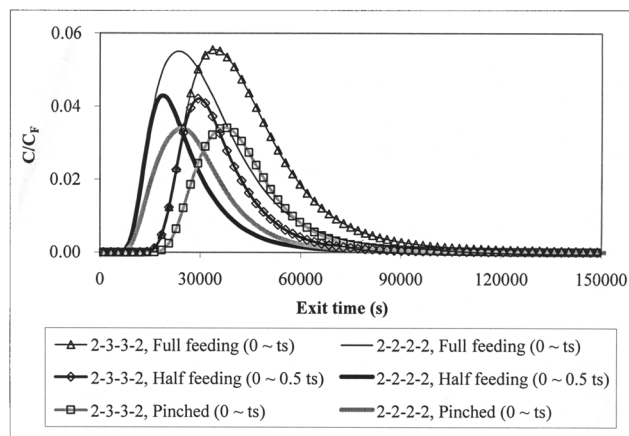


Figure 16. Comparison of all the proposed strategies to reduce the residence time of insulin in Ring II.

All the effluent histories were obtained from VERSE simulations and concentrations in the effluent history are averaged over one switching period. Unless otherwise noted, the operating conditions are based on the standing wave design.

the effluent history for a feed pulse over one switching period for each strategy is obtained from VERSE simulations. Figure 16 shows that either the partial feeding strategy or the pinched wave design based on shorter zone II and zone III lengths is the most effective in shortening the residence time of insulin in Ring II.

Conclusions

The residence time of insulin in a size-exclusion SMB process was investigated using two different approaches. The first approach was based on local equilibrium analysis, assuming negligible mass-transfer effects. Its simplicity made it possible to isolate the effects of port location and port movement from the effects of recycle. The second approach was based on simulations from a detailed rate model (VERSE), in which all the effects, including port location, port movement, recycle, and mass transfer, are considered. Comparison of the results from the two approaches shows the effects of mass transfer on residence time and RTD.

The RTD in SMB was found to be quite different from the RTD in batch chromatography. Unlike the RTD of batch chromatography, the RTD in SMB depends on the injection time as a result of the location of the product ports, periodic

Table 7. Residence Times of Insulin in Ring II from the Standing Wave Design, Partial Feeding Strategy, and Pinched Wave Design Based on Shorter Zone Lengths (2-2-2-2 Zone Configuration)

Ring II (2-2-2-2)	t_m	$t_{0.95}$	$t_{0.99}$
Standing wave design (100% throughput)	3.528×10^4 s (16.9 t_s)	7.128×10^4 s (34.2 t_s)	1.238×10^5 s (59.4 t_s)
Partial feeding strategy (50% throughput)	2.711×10^4 s (13.0 t_s)	5.256×10^4 s (25.2 t_s)	8.964×10^4 s (43.0 t_s)
Pinched wave design (50% throughput)	3.118×10^4 s (14.9 t_s)	5.760×10^4 s (27.6 t_s)	9.432×10^4 s (45.2 t_s)

* t_s of Ring II (2-2-2-2): 2.086×10^3 s.

port movement, recycle, and mass-transfer effects. There is a large difference between the residence time of a fast moving solute and that of a slow moving solute because the raffinate port is located downstream from the feed port, whereas the extract port is located upstream from the feed port. For a fast moving solute, the earlier it is injected during a switching period, the earlier it leaves SMB (first in, first out). This trend is reversed for a slow moving solute (first in, last out). Furthermore, solute molecules undergo multiple recycles in SMB. Each small pulse injected is split into a recycle pulse train with diminishing magnitude, as shown in the tracer analysis. The decay of the pulse train occurs more gradually (or long tailing in RTD), as more solutes are cycled. Mass-transfer effects broaden all the recycle pulse trains, resulting in longer residence times and broader residence time distribution. The longer a pulse stays in SMB, the more pronounced the mass-transfer effects.

If a smaller residence time is required for insulin stability, a partial feeding strategy can be used to shorten the residence time of insulin. In this strategy, the feed should be injected only during the second half-switching time in Ring I, and during the first half-switching time in Ring II. The pinched wave design can also shorten the residence time of insulin. In this design, the zone III flow rate in Ring I should be lower than the standing wave value and the zone II flow rate in Ring II should be higher than the standing wave value. VERSE simulation results confirm that both the partial feeding strategy and the pinched wave design significantly reduce the residence times of insulin. Decreasing the lengths of zone II in Ring I and zone III in Ring II also helps shorten the residence time of insulin. Either the partial feeding strategy or the pinched wave design can be used in combination with shorter zone lengths to further reduce the residence time of insulin.

Acknowledgments

This work was supported in part by NSF (0215146) and the 21st Century Research Grant from the State of Indiana. We are grateful to the Bioseparation Group at Purdue University for their valuable advice and suggestions. We also thank Dr. Fred Larimore from Eli Lilly and Company for raising the issue on solute residence time in SMB and inspiring this work.

Notation

a_i = linear equilibrium distribution coefficient of component i , $\text{m}^3/\text{m}^3 \text{ S.V.}$
 C = concentration, kg/m^3
 D_p = intraparticle diffusivity, m^2/s
 D_∞ = Brownian diffusivity, m^2/s
 DV = dead volume
 $E(t)$ = residence time distribution function
 E_b = axial dispersion coefficient, m^2/s
 F^j = flow rate in zone j , m^3/s
 F_p = product flow rate, m^3/s
 F_r = recycled flow rate, m^3/s
 k_f = film mass-transfer coefficient, m/s
 K_e = size exclusion factor
 L_c = length of a single column, m
 N_0 = total amount of solute injected into SMB
 N_{col}^j = number of columns in zone j
 $NR_R^{0.05}$ = number of recycles to remove 5% of solutes from SMB
 $NR_R^{0.95}$ = number of recycles to remove 95% of solutes from SMB
 N_f^{II} = smallest number of switchings such that the fast-moving solute no longer has access to zone II

N_f^{III} = number of additional switchings required for the fast-moving solute to reach the raffinate port after the N_f^{II} th switching
 N_s^{II} = number of additional switchings required for the slow moving solute to enter zone I after the N_s^{III} th switching
 N_s^{III} = smallest number of switchings such that the slow-moving solute no longer has access to zone III
 $P \equiv (1 - \epsilon_b)/\epsilon_b$ = phase ratio, or the volume ratio of the particle phase to the mobile phase
 rc = recycle ratio
 S = column cross-sectional area, m^2
 S.V. = solid volume, m^3
 t = time, s
 t_{in} = injection time, s
 t_m = mean residence time, s
 t_{min} = minimum residence time, s
 $t_{RC,n}$ = residence time after the n th recycle, s
 t_s = switching time, s
 $t_{0.05}$ = breakthrough time, s
 $t_{0.95}$ = extinction time, s
 t_0^I = amount of time that the slow-moving solute spends in zone I after the $(N_s^{III} + N_s^{II})$ th switching, s
 t_0^{III} = amount of time that the fast-moving solute spends in zone III after the $(N_f^{II} + N_f^{III} - 1)$ th switching, s
 u_0^j = interstitial velocity in zone j , $\text{m}/\text{s} = F^j/(\epsilon_b S)$
 $u_{s,i}^j$ = linear velocity of solute i in zone j , m/s
 $u_{w,i}^j$ = net linear velocity of solute i in zone j with respect to the feed port, m/s

Greek letters

$\delta_i \equiv K_{e,i} \epsilon_p + (1 - K_{e,i} \epsilon_p) a_i$ = retention factor of component i
 ΔN = amount of solute leaving SMB for a time period of Δt
 ϵ_b = interparticle void fraction
 ϵ_p = intraparticle void fraction
 v = average port velocity, m/s
 σ = standard deviation, s

Literature Cited

- Baker, J., *Finite Element Computational Fluid Dynamics*, McGraw-Hill, New York (1983).
 Berninger, J. A., R. D. Whitley, X. Zhang, and N.-H. L. Wang, "A Versatile Model for Simulation of Reaction and Nonequilibrium Dynamics in Multicomponent Fixed-Bed Adsorption Processes," *Comp. Chem. Eng.*, **15**, 749 (1991).
 Chung, S. F., and C. Y. Wen, "Longitudinal Dispersion of Liquid Flowing through Fixed and Fluidized Beds," *AIChE J.*, **14**, 857 (1968).
 Danckwerts, P. V., "Continuous Flow Systems: Distribution of Residence Times," *Chem. Eng. Sci.*, **2**, 1 (1953).
 Finlayson, B. A., *Nonlinear Analysis in Chemical Engineering*, McGraw-Hill, New York (1980).
 Fogler, H. S., *Elements of Chemical Reaction Engineering*, Prentice-Hall, Englewood Cliffs, NJ (1986).
 Hritzko, B. J., "Design and Dynamic Modeling of Simulated Moving Bed Process for Multicomponent Biochemical Separations," PhD Diss., Dept. of Chemical Engineering, Purdue University, West Lafayette, IN (2001).
 Hritzko, B. J., Y. Xie, R. J. Wooley, and N.-H. L. Wang, "Standing Wave Design of Tandem SMB for Linear Multicomponent Systems," *AIChE J.*, **48**, 2769 (2002).
 Kroeft, E. P., R. A. Owens, E. L. Campbell, R. D. Johnson, and H. I. Marks, "Production Scale Purification of Biosynthetic Human Insulin by Reversed-Phase High-Performance Liquid Chromatography," *J. Chromatogr.*, **45**, 461 (1989).
 Ladisch, M. R., and K. L. Kohlmann, "Recombinant Human Insulin," *Biotechnol. Prog.*, **8**, 469 (1992).
 Levenspiel, O., *Chemical Reaction Engineering*, Wiley, New York (1972).
 Ma, Z., and N.-H. L. Wang, "Standing Wave Analysis of SMB Chromatography: Linear Systems," *AIChE J.*, **43**, 2488 (1997).

- Ma, Z., R. D. Whitley, and N.-H. L. Wang, "Pore and Surface Diffusion in Multicomponent Adsorption and Liquid Chromatography Systems," *AIChE J.*, **42**, 1244 (1996).
- Petzold, L. R., "Description of DASSL: A Differential/Algebraic System Solver," Lawrence Livermore National Laboratories, Technical Report SAND-82-8637 (1982).
- Villadsen, J. V., and M. L. Michelsen, *Solution of Differential Equation Model by Polynomial Approximation*, Prentice-Hall, Englewood Cliffs, NJ (1978).
- Wankat, P. C., *Rate-Controlled Separations*, Blackie, Glasgow/London (1994).
- Whitley, R. D., "Dynamics of Nonlinear Multicomponent Chromatography-Interplay of Mass Transfer, Intrinsic Sorption Kinetics, and Reaction," PhD Diss., Dept. of Chemical Engineering, Purdue University, West Lafayette, IN (1990).
- Wilson, E. J., and C. J. Geankoplis, "Liquid Mass Transfer at Very Low Reynolds Numbers in Packed Beds," *Ind. Eng. Chem. Fundam.*, **5**, 9 (1966).
- Xie, Y., S. Mun, J.-H. Kim, and N.-H. L. Wang, "Standing Wave Design and Experimental Validation of a Tandem Simulated Moving Bed Process for Insulin Purification," *Biotechnol. Prog.*, **18**, 1332 (2002).

Appendix: Derivation of Residence Time Based on a Local Equilibrium Model

See Figure A1. The position of the feed port is set to be 0. The traveling distance of a solute has a positive sign while the solute is moving downstream from the feed port, but a negative sign while the solute is moving upstream. The residence time of a solute corresponds to the amount of time spent for moving from $z = 0$ to $z = -N_{col}^{III} \cdot L_c$ or $N_{col}^{III} \cdot L_c$.

First, we derive the residence time of a slow-moving solute (extract product). The entire paths experienced by the solute can be divided into three groups as shown in Figure A2.

$T_{(II \leftrightarrow III)}$ is the amount of time the solute spends in SMB until it no longer has access to zone III. $T_{(II)}$ is the amount of time the solute spends in zone II until it enters zone I. $T_{(I)}$ is the amount of time the solute spends in zone I until it exits the extract port. The residence time of the solute in SMB is the sum of $T_{(II \leftrightarrow III)}$, $T_{(II)}$, and $T_{(I)}$. The solute injected at time t_{in} migrates in zone III in the positive direction. After the first switching, the solute enters zone II and its position is given by $[(t_s - t_{in}) \cdot u_{s2}^{III} - L_c]$. During the second step (between the first switching and the second switching), the solute travels toward zone III. If the amount of time required to reach zone III (t_1^{II}) is smaller than t_s , the position of the solute after the second switching is given by

$$(t_s - t_{in}) \cdot u_{s2}^{III} - L_c + t_1^{II} \cdot u_{s2}^{II} + (t_s - t_1^{II}) \cdot u_{s2}^{III} - L_c \quad (A1)$$

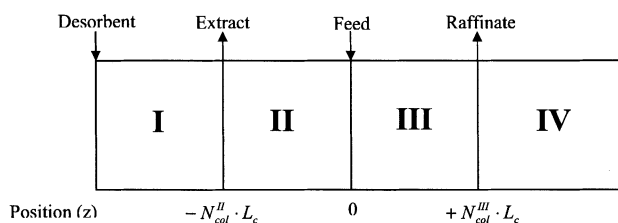


Figure A1. Position of each port in SMB.

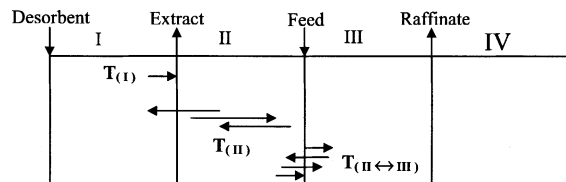


Figure A2. Traveling path of a slow-moving solute in SMB.

where $t_0^{II} \equiv t_{in}$ and $t_1^{II} =$

$$\frac{-(t_s - t_0^{II}) \cdot u_{s2}^{III} - L_c}{u_{s2}^{II}} \quad (A2)$$

After the second switching, the solute enters zone II and travels toward zone III again during the third step. If the amount of time required to reach zone III (t_2^{II}) is smaller than t_s , the position of the solute after the third switching is given by

$$(t_s - t_{in}) \cdot u_{s2}^{III} - L_c + \sum_{i=1}^2 [t_i^{II} \cdot u_{s2}^{II} + (t_s - t_i^{II}) \cdot u_{s2}^{III} - L_c] \quad (A3)$$

where

$$t_2^{II} = \frac{-(t_s - t_{in}) \cdot u_{s2}^{III} - L_c + \sum_{i=1}^1 [t_i^{II} \cdot u_{s2}^{II} + (t_s - t_i^{II}) \cdot u_{s2}^{III} - L_c]}{u_{s2}^{II}} \\ = t_1^{II} - \frac{\sum_{i=1}^1 [t_i^{II} \cdot u_{s2}^{II} + (t_s - t_i^{II}) \cdot u_{s2}^{III} - L_c]}{u_{s2}^{II}} \quad (A4)$$

If we repeat the above procedure N times, the position of the solute after the N th switching results in

$$(t_s - t_{in}) \cdot u_{s2}^{III} - L_c + \sum_{i=1}^{N-1} [t_i^{II} \cdot u_{s2}^{II} + (t_s - t_i^{II}) \cdot u_{s2}^{III} - L_c] \quad (A5)$$

where t_0^{II} and t_1^{II} are determined from Eq. A2. In addition

$$t_k^{II} = t_1^{II} - \frac{\sum_{i=1}^{k-1} [t_i^{II} \cdot u_{s2}^{II} + (t_s - t_i^{II}) \cdot u_{s2}^{III} - L_c]}{u_{s2}^{II}} \quad (k \geq 2) \quad (A6)$$

If N_s^{III} is defined as the smallest N such that t_N^{II} is larger than t_s , the solute no longer has access to zone III after the N_s^{III} th switching. Therefore, the amount of time the solute

spends in SMB until the N_s^{III} th switching corresponds to $T_{(II \leftrightarrow III)}$, which is the sum of the times in Eq. A5 as follows

$$T_{(II \leftrightarrow III)} = (t_s - t_{in}) + t_s \cdot (N_s^{III} - 1) \quad (A7)$$

To simplify the expression for the position of the solute at time $T_{(II \leftrightarrow III)}$, we rearrange Eq. A5 and substitute Eq. A6 into Eq. A5 as follows

(The position of the solute at time $T_{(II \leftrightarrow III)}$)

$$\begin{aligned} &= (t_s - t_{in}) \cdot u_{s2}^{III} - L_c + \sum_{i=1}^{N_s^{III}-1} [t_i^{II} \cdot u_{s2}^{II} + (t_s - t_i^{II}) \cdot u_{s2}^{III} - L_c] \\ &= (t_s - t_{in}) \cdot u_{s2}^{III} - L_c + \sum_{i=1}^{N_s^{III}-2} [t_i^{II} \cdot u_{s2}^{II} + (t_s - t_i^{II}) \cdot u_{s2}^{III} - L_c] \\ &\quad + t_{N_s^{III}-1}^{II} \cdot u_{s2}^{II} + (t_s - t_{N_s^{III}-1}^{II}) \cdot u_{s2}^{III} - L_c \\ &= (t_s - t_{in}) \cdot u_{s2}^{III} - L_c + \sum_{i=1}^{N_s^{III}-2} [t_i^{II} \cdot u_{s2}^{II} + (t_s - t_i^{II}) \cdot u_{s2}^{III} - L_c] + \\ &\quad - \left\{ (t_s - t_{in}) \cdot u_{s2}^{III} - L_c + \sum_{i=1}^{N_s^{III}-2} [t_i^{II} \cdot u_{s2}^{II} + (t_s - t_i^{II}) \cdot u_{s2}^{III} - L_c] \right\} \cdot \frac{u_{s2}^{II}}{u_{s2}^{III}} \end{aligned}$$

$$u_{s2}^{II} + (t_s - t_{N_s^{III}-1}^{II}) \cdot u_{s2}^{III} - L_c = (t_s - t_{N_s^{III}-1}^{II}) \cdot u_{s2}^{III} - L_c \quad (A8)$$

After the N_s^{III} th switching, the solute migrates in zone II. To enter zone I, additional N_s^{II} switchings are needed and determined as follows

(The position of the solute at time $\{T_{(II \leftrightarrow III)} + T_{(II)}\}$)

$$\begin{aligned} &= (\text{The position of the solute at time } T_{(II \leftrightarrow III)}) + u_{s2}^{II} \cdot t_s \\ &\quad \cdot N_s^{II} - N_s^{II} \cdot L_c < -N_{col}^{II} \cdot L_c \quad (A9) \end{aligned}$$

Substitution of Eq. A8 into Eq. A9 gives

$$N_s^{II} > \frac{(t_s - t_{N_s^{III}-1}^{II}) \cdot u_{s2}^{III} + (N_{col}^{II} - 1) \cdot L_c}{L_c - t_s \cdot u_{s2}^{II}} \quad (A10)$$

The smallest N_s^{II} that satisfies Eq. A10 is used to calculate $T_{(II)}$

$$T_{(II)} = t_s \cdot N_s^{II} \quad (A11)$$

After the $(N_s^{III} + N_s^{II})$ th switching, the solute exits the extract port within one switching period. Let t_0^I be the amount of time the solute spends in zone I until it exits the extract port. The t_0^I is obtained by equating the position of the extract port with the position of the solute.

$$(\text{The position of the extract port}) = (\text{The position of the solute at time } \{T_{(II \leftrightarrow III)} + T_{(II)}\}) + t_0^I \cdot u_{s2}^I = -N_{col}^{II} \cdot L_c \quad (A12)$$

Solving Eq. A12 for the t_0^I gives

$$t_0^I = \frac{(L_c - t_s \cdot u_{s2}^{II}) \cdot N_s^{II} - (t_s - t_{N_s^{III}-1}^{II}) \cdot u_{s2}^{III} - (N_{col}^{II} - 1) \cdot L_c}{u_{s2}^I} \quad (A13)$$

$$T_{(I)} = t_0^I \quad (A14)$$

Finally, the residence time of the solute without recycle in SMB (t_{min}) is obtained from the sum of times $T_{(II \leftrightarrow III)}$, $T_{(II)}$, and $T_{(I)}$.

$$t_{min} = (t_s - t_{in}) + t_s \cdot [(N_s^{III} - 1) + N_s^{II}] + t_0^I \quad (A15)$$

If the solute is recycled back to zone II, the solute spends a time period of $(t_s - t_0^I)$ in zone II and moves into zone I after port switching. Let t_1^I be the amount of time the solute spends in zone I after the first recycle. The t_1^I is determined by equating the position of the extract port with the position of the solute as follows

$$-N_{col}^{II} \cdot L_c + (t_s - t_0^I) \cdot u_{s2}^{II} - L_c + t_1^I \cdot u_{s2}^I = -N_{col}^{II} \cdot L_c \quad (A16)$$

Solving Eq. A16 for t_1^I gives

$$t_1^I = \frac{L_c - (t_s - t_0^I) \cdot u_{s2}^{II}}{u_{s2}^I} \quad (A17)$$

Therefore, the residence time of the solute after the first recycle ($t_{RC,1}$) is given by

$$t_{RC,1} = t_{RC,0} + (t_s - t_0^I) + t_1^I \quad (A18)$$

where $t_{RC,0} \equiv t_{min}$

If the above procedure is repeated, the residence time of the solute after the n th recycle ($t_{RC,n}$) is given by

$$t_{RC,n} = t_{RC,n-1} + (t_s - t_{n-1}^I) + t_n^I \quad (A19)$$

where

$$t_n^I = \frac{L_c - (t_s - t_{n-1}^I) \cdot u_{s2}^{II}}{u_{s2}^I} \quad (n \geq 1) \quad (A20)$$

Plugging serial numbers into Eq. A19, one has the following equations in series

$$\begin{aligned} t_{RC,n} &= t_{RC,n-1} + (t_s - t_{n-1}^I) + t_n^I \\ t_{RC,n-1} &= t_{RC,n-2} + (t_s - t_{n-2}^I) + t_{n-1}^I \\ &\vdots \\ t_{RC,1} &= t_{RC,0} + (t_s - t_0^I) + t_1^I \end{aligned}$$

Addition of all the equations above gives

$$t_{RC,n} = t_{RC,0} + n \cdot t_s - t_0^I + t_n^I \quad (\text{A21})$$

Since t_n^I is a function of t_{n-1}^I , t_{n-2}^I , and so on, Eq. A21 still requires sequential calculations as presented below. To derive the explicit expression for t_n^I , we first subtract t_{n-1}^I from t_n^I and plug serial numbers into the resulting equation as follows

$$\begin{aligned} t_n^I - t_{n-1}^I &= (t_{n-1}^I - t_{n-2}^I) \cdot (u_{s2}^{II}/u_{s2}^I) \\ t_{n-1}^I - t_{n-2}^I &= (t_{n-2}^I - t_{n-3}^I) \cdot (u_{s2}^{II}/u_{s2}^I) \\ &\vdots \\ t_2^I - t_1^I &= (t_1^I - t_0^I) \cdot (u_{s2}^{II}/u_{s2}^I) \end{aligned}$$

Multiplication of all the equations above gives

$$t_n^I - t_{n-1}^I = (t_1^I - t_0^I) \cdot (u_{s2}^{II}/u_{s2}^I)^{n-1} \quad (\text{A22})$$

Plugging the numbers of n into Eq. A22, one has the following equations in series

$$\begin{aligned} t_n^I - t_{n-1}^I &= (t_1^I - t_0^I) \cdot (u_{s2}^{II}/u_{s2}^I)^{n-1} \\ t_{n-1}^I - t_{n-2}^I &= (t_1^I - t_0^I) \cdot (u_{s2}^{II}/u_{s2}^I)^{n-2} \\ &\vdots \\ t_1^I - t_0^I &= (t_1^I - t_0^I) \end{aligned}$$

Addition of all the equations above gives

$$t_n^I - t_0^I = (t_1^I - t_0^I) \cdot \left[1 + \left(\frac{u_{s2}^{II}}{u_{s2}^I} \right) + \cdots + \left(\frac{u_{s2}^{II}}{u_{s2}^I} \right)^{n-2} + \left(\frac{u_{s2}^{II}}{u_{s2}^I} \right)^{n-1} \right] \quad (\text{A23})$$

Finally, t_n^I is expressed into t_0^I and t_1^I as follows

$$t_n^I = t_0^I + (t_1^I - t_0^I) \cdot \left(\frac{1 - (u_{s2}^{II}/u_{s2}^I)^n}{1 - (u_{s2}^{II}/u_{s2}^I)} \right) \quad (\text{A24})$$

Substitution of Eq. A24 into Eq. A21 results in the final expression for $t_{RC,n}$

$$t_{RC,n} = t_{RC,0} + n \cdot t_s + (t_1^I - t_0^I) \cdot \left(\frac{1 - (u_{s2}^{II}/u_{s2}^I)^n}{1 - (u_{s2}^{II}/u_{s2}^I)} \right) \quad (\text{A25})$$

Similarly, the residence time of a fast-moving solute (raffinate product) can also be derived. Taking the same procedures as in a slow-moving solute, one can obtain the mathematical expression for the residence time of the fast-moving solute. Below is the minimum residence time of the fast-moving solute (t_{\min})

$$t_{\min} = (t_s - t_{in}) + t_s \cdot [(N_f^{II} - 1) + (N_f^{III} - 1)] + t_0^{III} \quad (\text{A26})$$

where N_f^{II} is the smallest N that satisfies the following equation

$$(t_s - t_{N-1}^{II}) \cdot u_{s1}^{III} - L_c > 0 \quad (\text{A27})$$

where t_{N-1}^{II} are calculated from the following two equations

$$t_0^{II} \equiv t_{in}, \quad t_1^{II} = \frac{L_c - (t_s - t_0^{II}) \cdot u_{s1}^{III}}{u_{s1}^{II}} \quad (\text{A28})$$

$$t_k^{II} = t_1^{II} - \frac{\sum_{i=1}^{k-1} [t_i^{II} \cdot u_{s1}^{II} + (t_s - t_i^{II}) \cdot u_{s1}^{III} - L_c]}{u_{s1}^{II}} \quad (k \geq 2) \quad (\text{A29})$$

The other terms in Eq. A26, N_f^{III} and t_0^{III} are determined by

$$N_f^{III} = \text{Integer} \left(\frac{N_{\text{col}}^{III} \cdot L_c - (t_s - t_{N_f^{II}-1}^{II}) \cdot u_{s1}^{III} + |N_{\text{col}}^{III} \cdot L_c - (t_s - t_{N_f^{II}-1}^{II}) \cdot u_{s1}^{III}|}{2 \times (t_s \cdot u_{s1}^{III} - L_c)} \right) \quad (\text{A30})$$

$$t_0^{III} = \frac{N_{\text{col}}^{III} \cdot L_c + N_f^{III} \cdot (L_c - t_s \cdot u_{s1}^{III}) + t_{N_f^{II}-1}^{II} \cdot u_{s1}^{III}}{u_{s1}^{III}} \quad (\text{A31})$$

where the operator “Integer” is used to round up the value inside parenthesis.

Furthermore, the residence time of the fast-moving solute after the n th recycle ($t_{RC,n}$) is calculated from

$$t_{RC,n} = t_{RC,0} + n \cdot t_s + (t_1^{III} - t_0^{III}) \cdot \left(\frac{1 - (u_{s1}^{IV}/u_{s1}^{III})^n}{1 - (u_{s1}^{IV}/u_{s1}^{III})} \right) \quad (\text{A32})$$

where

$$t_{RC,0} \equiv t_{\min} \quad \text{and} \quad t_1^{III} = \frac{L_c - (t_s - t_0^{III}) \cdot u_{s1}^{IV}}{u_{s1}^{III}} \quad (\text{A33})$$

Manuscript received Sept. 13, 2002, and revision received Apr. 28, 2003.